Contribution of Electrostatic Cohesive Energy in Two-Dimensional J-Aggregation of Cyanine Dye

Mitsuo Kawasaki* and Hisao Inokuma

Department of Molecular Engineering, Graduate School of Engineering, Kyoto University, Yoshida, Kyoto 606-8501, Japan

Received: September 16, 1998; In Final Form: December 7, 1998

Well-ordered two-dimensional (2D) J-aggregates of cyanine dyes can be easily self-assembled on an atomically flat Ag(111) film covered with a halide monolayer, thus serving as a superior model system for studying the 2D J-aggregation of cyanine dyes. The 2D J-aggregate structure of a thiacarbocyanine dye has been examined in detail by optical absorption spectroscopy, X-ray photoelectron spectroscopy (XPS), and kinetic analysis of molecular desorption in dye solvent. An angle-resolved XPS allowed easy determination of the vertical molecular orientation in the 2D J-aggregate. More importantly, an intramolecular chemical shift near 1 eV at maximum between the cationic dye chromophore and the counteranion, together with the kinetic information concerning the solvent-induced molecular desorption, illuminated the dominant contribution of an electrostatic Madelung energy to the overall cohesive energy for 2D J-aggregation. This collective Coulomb interaction also gives strong constraint in respect to the type of 2D molecular network so that only J-aggregation becomes energetically feasible in the case of the selected thiacarbocyanine dye.

1. Introduction

Cyanine dyes, which are known as an important spectral sensitizer in photographic materials,[1] form a variety of molecular aggregates with diverse spectral properties. Among others, an unusually sharp and fluorescent electronic transition that significantly red-shifted from the monomer band, referred to as the J-band, is the most prominent new spectral feature arising from such a molecular aggregation of cyanine dyes. There has been much theoretical interest in the excitation energy transfer and the radiative decay kinetics in J-aggregates.[2−4] Practically, along with their established use in photographic materials, frequent mention has also been made of their potential use for nonlinear optical materials.[5,6]

According to the earlier theoretical calculation of Norland, Ames, and Tayler based on the molecular exciton theory,[7] the exact transition energy of dye aggregate is a sensitive function of the so-called slip angle (the angle between the molecular long axis and the line of centers of stacked molecules) and the J-band is attributed to close-packed cyanine molecules stacked plane-to-plane with a sufficiently small slip angle less than 32°. This criterion, however, tells us nothing about the reason some specific slip angle occurs in each dye aggregate—a question intimately correlated with what determines the molar cohesive energy of J-aggregate. In this respect the only quantitative data reported in the literature are the limited thermodynamic parameters for J-aggregation in aqueous solution. On the basis of the analysis of solution equilibria between monomers and J-aggregates (reportedly composed of 4−8 dye molecules) for a couple of carbocyanine dyes,[8,9] it has been suggested that the association enthalpy per mol-monomers for the J-aggregation in solution may be typically ∼42 kJ/mol (∼0.4 eV). Yet this value, which is for such an embryonic J-aggregate in solution, is by no means applicable to the more interesting form of layered J-aggregate on solid surfaces, as found in photographic materials (adsorbed on AgX microcrystals) and also in composite LB (Langmuir−Blodgett) monolayers.

The LB technique has indeed been extensively used to prepare thin films of layered J-aggregates, which have been assumed to form a virtual, two-dimensional (2D) crystal, preferably with a brickstone arrangement of the dye chromophores.[10,11] This particular arrangement has been tested favorably by means of electron diffraction,[12] second-harmonic generation,[13] and scanning force microscopy,[14] and in fact satisfies the aforementioned slip-angle criterion. It is desirable, however, to have a model 2D J-aggregate even simpler both in structure and in preparation than that in LB films to inquire further into some of the most fundamental aspects of the physics and chemistry involved in 2D aggregation of cyanine dyes. What seems particularly useful from this standpoint are the 2D J-aggregates that can be easily self-assembled without assistance of amphiphilic monolayers on a large-area, atomically flat, Ag(111) film covered with a halide monolayer.[15,16]

The halide-covered Ag(111) surface has been proved to resemble (never identical with) both chemically and structurally the (111) surface of silver halides.[15,16] Thus a variety of cyanine dyes that are known to be adsorbed well on AgX surfaces are expected to be adsorbed equally well on the halide-covered Ag(111). Furthermore a well-ordered 2D molecular network on the highly planar pseudo-AgX model surface, with its outstanding structural simplicity, allows a variety of structural characterizations by combined physical and/or chemical methods. In this paper we describe a combination of optical absorption spectroscopy, X-ray photoelectron spectroscopy (XPS), and kinetic analysis of solvent-induced molecular desorption that enabled us to find a large contribution of collective Coulomb interaction (or Madelung energy) involving the cationic dye chromophores and the counteranions to the overall cohesive energy for 2D J-aggregation. Importance of this kind of electrostatic energy may even intuitively be predictable, but

* Corresponding author. Fax: (+81)-75-753-5526. E-mail: kawasaki@ap6.kuic.kyoto-u.ac.jp.

10.1021/jp983736f CCC: $18.00
Published on Web 02/05/1999

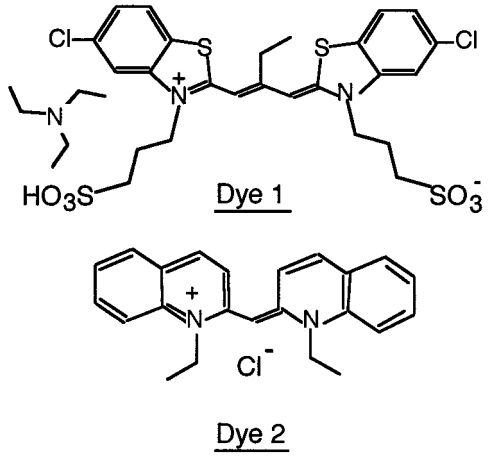

Figure 1. Molecular structures of cyanine dyes used in this work.

nevertheless has been given rather minor attention and no quantitative consideration whatsoever.

2. Experimental Section

2.1. Materials and Self-Assembly Procedure. A simple DC glow-discharge sputtering method to prepare atomically flat Ag(111)/Au(111) films on mica has been described in detail elsewhere.[15,17,18] It has been suggested that a low-energy Ar-ion bombardment of the growing film surface with maximum allowed kinetic energies of several electronvolts makes an important contribution to the marked flatness of the Ag(111) film.[18] When grown in the optimum conditions, the Ag(111) film surface has an extensively terraced texture with a typical monatomic terrace width easily exceeding hundreds of nanometers.

Once exposed to the ambient atmosphere, the as-grown Ag(111) film is immediately covered by a native oxide monolayer. This can be readily replaced by a halide monolayer by simply bathing the film in a dilute alkali halide solution. Used in this work for this purpose was 10^{-3} M KBr (MERCK, Suprapure reagent) in a mixed solvent of singly distilled water and ethanol (Nacalai Tesque, Inc., guaranteed reagent) of 1:1 volume ratio. The bathing time and temperature were typically 5 min and 20 °C, but the bathing conditions are not critical at all to obtain the bromide-covered Ag(111). It should be also noted that no potassium ions (contained as the countercations in the KBr solution) have been detected by XPS on the thus bromide-covered surface,[15] in agreement with the above-noted substitutional oxide-to-halide conversion mechanism for the bromide formation.

Thiacarbocyanine dye (Dye 1), 5,5′-dichloro-3,3′-disulfopropyl-9-ethyl-thiacarbocyanine triethylamine, was kindly supplied by Dr. Rene De Keyzer (Agfa Gevaert N. V., Belgium). Simple cyanine (Dye 2), 1,1′-diethyl-2,2′-cyanine chloride, was purchased from Nippon Kanko Shikiso Co. The structures of these dyes are shown in Figure 1 in the most probable (see the related discussion given later) conformation that occurs in 2D dye aggregates. In this work Dye 2 was used primarily as a diluent, which by being coadsorbed with Dye 1 alters the average size of the 2D J-aggregate of Dye 1. These dyes were used in the form of 10^{-4} M solution (including mixed solutions of Dye 1 and Dye 2) in the mixed water and ethanol solvent of 1:1 volume ratio. 2D J-aggregates were easily self-assembled on the bromide-covered Ag(111) in these solutions well within a minute at room temperature. The film was then quickly rinsed by cooled pure water and allowed to dry after visible water droplets had been blown off.

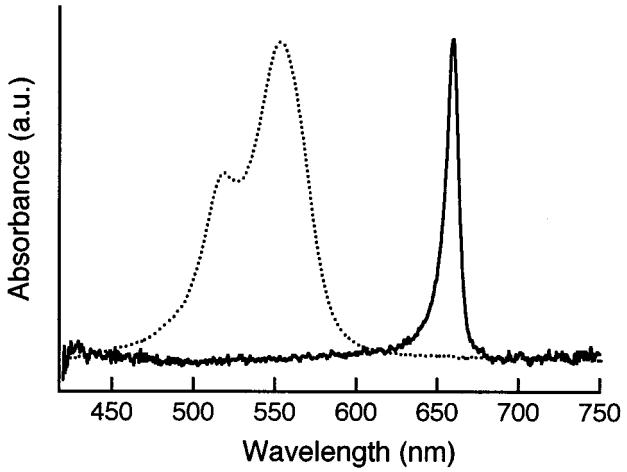

Figure 2. Absorption spectrum (solid line) of self-assembled 2D J-aggregate of Dye 1 on a bromide-covered Ag(111). A spectrum (dotted line) taken for a monomeric dye solution is included for reference. The intensity is normalized to the peak reflection absorbance, 0.058, for the 2D J-aggregate and to the peak absorbance, 0.11, for the 10^{-6} M monomer solution with 1 cm path length.

2.2. Absorption Spectroscopy and Desorption Experiment. The bromide-covered Ag(111) film used in this work is nontransparent and has a highly reflective mirrorlike surface. Thus the absorption spectra of the 2D J-aggregate self-assembled thereupon were taken in the reflection mode (at normal incidence) by using a spectromicroscope, comprising a multichannel analyzer PMA-11 (Hamamatsu Co.) and a Nikon microscope. Here the spectrum is given in terms of the reflection absorbance as defined by $\log(R_0/R)$, where R and R_0 represent the measured reflectance of the sample with and without the adsorbed dye, respectively. The microscope was operated under the lowest magnification of $\times 10$, the corresponding sampling spot diameter being typically ~ 1 mm.

Three kinds of solvents—water, ethanol, and mixed water and ethanol of 1:1 volume ratio—were used for the desorption experiment. The 2D J-aggregate on the bromide-covered Ag(111) film, typically 3×8 mm^2, was brought into an excess amount of each solvent, ~ 20 mL in volume, being constantly stirred and maintained at a controlled temperature. After any desired period of this treatment the sample was quickly removed from the solvent bath, dried by air jet, and then subjected again to the reflection spectroscopy analysis. Changes in the intensity and the shape of the J-band as functions of time in the solvent thus provide useful kinetic information about the molecular desorption from the 2D J-aggregate.

2.3. XPS Analysis. All XPS data were taken in an ESCA-750 spectrometer (Shimazu Corp.) with Mg Kα radiation of 1253.6 eV. The sample size was typically $\sim 6 \times 6$ mm^2. The angle-resolved spectra were taken for three different photoemission angles, 90°, 30°, and 10° with respect to the sample plane. The binding energy of each signal was determined by referring to the peak of the N_{1s} signal, associated with the heterocyclic ring of the main dye chromophore, as the common internal reference being placed at the fixed position of 401 eV.

3. Results and Discussion

3.1. Absorption Characteristics. Figure 2 (solid line) shows a typical absorption spectrum of the 2D J-aggregate of Dye 1 that has been self-assembled on the bromide-covered Ag(111) film. As mentioned already the rate of self-assembly was so large that complete monolayer coverage of the substrate was reached well within a minute in the 10^{-4} M dye solution. That

only a single dye monolayer is allowed to form in this process is supported by the fact that longer treatment caused no further change in the spectrum and that identical spectra (both in shape and intensity) were obtained at much lower (10^{-5} M) and higher (10^{-3} M) dye concentrations as well. In Figure 2, comparison with the dotted curve, a reference spectrum taken for a monomeric dye solution, immediately lets us know a large red-shift (by ~100 nm) from the monomer band and a marked narrowing (~10 nm bandwidth at half-maximum) characteristic of the J-band. It is known that Dye 1 and its close analogues have a strong tendency for J-aggregation, but the 10 nm bandwidth observed here is exceptionally small as compared to those (>20 nm) previously reported for similar 2D J-aggregates but formed in AgBr emulsions[19,20] or in LB films.[21,22] Furthermore the J-band shown in Figure 2 exhibits no other sidebands. These facts indicate that the adsorbed dye molecules have been organized into some particularly well-defined J-aggregate structure. It should be also noted that the intensity of the J-band was invariant over the whole area of the film surface, thus ensuring that the substrate had been entirely and uniformly covered by the 2D J-aggregate. All of these features can be associated with the superior flatness of the substrate. In fact, inhomogeneous broadening of the J-band (>20 nm in bandwidth) could be easily found on atomically much rougher Ag(111) substrates that had been grown without care in away from the optimum deposition condition.

Such a uniform structure of the 2D J-aggregate achieved on the highly planar substrate allows the fractional area of the substrate occupied by each dye molecule to be determined simply by measuring the total number of dye molecules per unit projectional area of the substrate, by means of, for example, a complete ethanolic extraction of the adsorbed dye molecules followed by routine spectrophotometric analysis of the resulting dye solution. The molecular area estimated in this way was ~80 Å^2 (1.3×10^{14} molecules/cm^2), which will be used later for discussion of the relevant molecular arrangement. Of course, if some fraction of the J-aggregate were present in a multilayer configuration, the average molecular area could be significantly greater than 80 Å^2 for the given dye coverage (1.3×10^{14} molecules/cm^2). However, the corresponding looser and less-uniform packing of dye molecules is not consistent with the very sharp J-band, nor with the high reproducibility of the absorption spectrum as mentioned above. The picture that our 2D J-aggregate forms a single dye monolayer on the bromide-covered Ag(111) also leads to most straightforward interpretation of all the other experimental results discussed below.

One may expect that the absolute dye coverage on the substrate (1.3×10^{14} molecules/cm^2) should also have some direct correlation with the intensity of the J-band that appeared in Figure 2. To establish this correlation, however, we need to go into further details about what the measured reflection absorbance really means. Obviously this quantity is never equivalent to what one might expect to obtain in the condition where the 2D J-aggregate simply interacts twice with the probe light, first with the incident and then with the reflected beam. One straightforward approach to the problem would be to apply the Fresnel formula to calculate the absolute reflectance for a very thin layer of light-absorbing species on the bromide-covered Ag(111) film, by assuming some equivalent optical constant (complex refractive index) and layer thickness appropriate for the 2D J-aggregate (the existence of the underlying bromide monolayer may be negligible in this and the following model). An alternative model, by which the underlying physics may be easier to understand, is to assume that the light absorption by the 2D J-aggregate occurs by its interaction with the standing wave that is set up as a result of the interference between the incident and reflected beams,[23] which have approximately equal intensities because the reflectance at the metallic Ag surface exceeds 0.95 in the visible region. The intensity of this standing wave (square amplitude of the total electric field) depends on the phase change upon reflection, which can be calculated[24] from the known refractive index (complex) of Ag[25] and that of the adlayer (assumed to be real; 1.3−1.4 for typical organic layers). In the region of the sharp J-band centered at 660 nm, for example, this calculation predicts a partially destructive interference at the reflecting plane, leading to the effective square amplitude of the electric field smaller by a factor of 0.35 as compared to that of the incident wave at normal incidence. This means that the light absorption by the 2D J-aggregate on the metallic Ag surface becomes substantially smaller than in the case where the same aggregate is allowed to interact with only the incident or reflected wave. An independent analysis based on the Fresnel formula, though not being detailed here, also suggested that the reflection absorbance of a thin absorbing layer (with a Lorenzian absorption line shape modeling the J-band at 660 nm) on Ag becomes smaller by a factor of 0.31−0.36 than the ordinary transmission absorbance of the same layer but placed in a transparent dielectric medium with a refractive index of 1.3−1.5, in reasonable agreement with the standing wave model.

Knowing the above meaning of the reflection absorbance, we can then make a quantitative comparison between the 2D J-band on Ag(111) and the monomer band in solution. First the integrated (over the wavenumber) absorbance for the monomer band in solution divided by the total number of molecules in the light path per unit area, a quantity proportional to the so-called oscillator strength, is calculated to be $2.79 \times 10^{-13} \times 1.5$ ($= 4.18 \times 10^{-13}$) cm/molecule. Here the factor 1.5 has been included to correct for the orientational difference that the monomer transition dipoles in solution have totally random orientations, whereas those in the 2D J-aggregate should be oriented in the direction parallel to the substrate surface. Next the integrated reflection absorbance for the 2D J-band divided by the measured dye coverage, 1.3×10^{14} molecules/cm^2, was found to be 1.44×10^{-13} cm/molecule. Dividing this further by the aforementioned factor of 0.31−0.36, correlating the reflection absorbance to the ordinary transmission absorbance, we get $4.0-4.6 \times 10^{-13}$ cm/molecule, which satisfactorily agrees with that (4.18×10^{-13} cm/molecule) of the monomer band in solution. This means that the total oscillator strength for the monomer band in solution is conserved in that of the 2D J-aggregate on Ag(111). This reasonable correlation strengthens the validity of the absolute dye coverage measured by the ethanolic extraction, and conversely provides a way to estimate the dye coverage from the integrated reflection absorbance.

When Dye 1 was coadsorbed with Dye 2 from their mixed dye solution, the J-band associated with Dye 1 was seriously deformed as shown in Figure 3. Here the molar percentage of Dye 2 in the mixed solution varies from 5 to 100%, the total dye concentration being maintained at 10^{-4} M. It should be noted here that while Dye 1 retains a good planarity in its conjugated dye chromophore, Dye 2 has a twisted molecular structure because of the intramolecular steric repulsion between the two H atoms at 3- and 3′-positions.[26] It is thus unlikely that Dye 1 and Dye 2 are mixed uniformly on a molecular level in the 2D dye assembly. Much more realistically Dye 2 acts as an effective diluent in such a way that the 2D J-aggregate of Dye 1 breaks up into smaller and smaller patches of 2D islands with

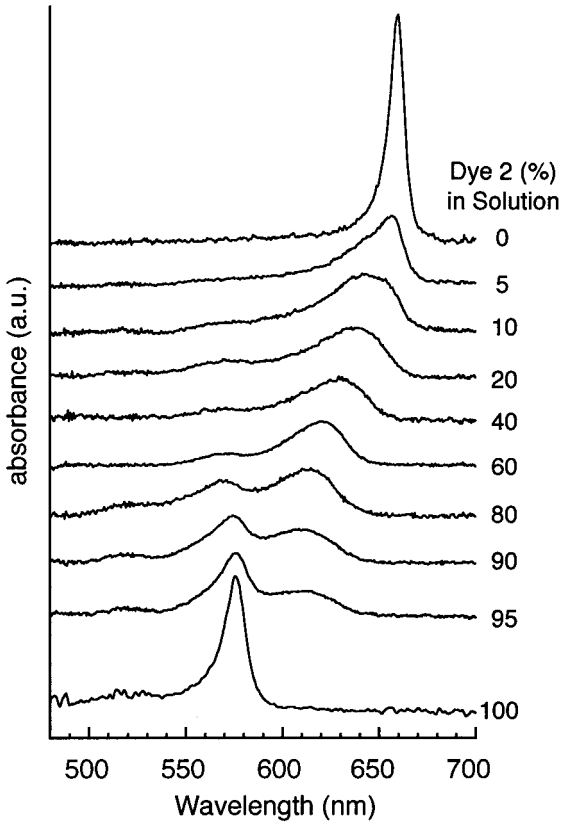

Figure 3. Series of absorption spectra taken for mixed 2D assemblies of Dye 1 and Dye 2 coadsorbed from mixed dye solutions. Numbers show molar percentage of Dye 2 in solution. The intensity is normalized to the same scale.

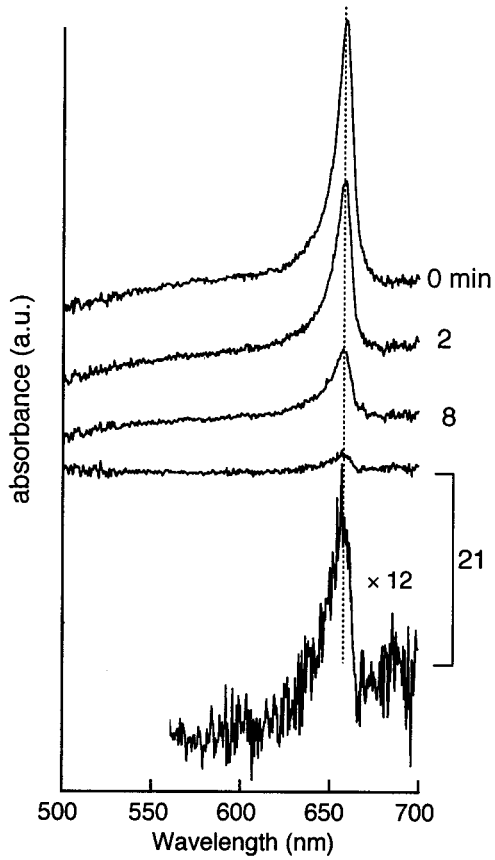

Figure 4. Change of J-band caused by molecular desorption from 2D J-aggregate of Dye 1 in mixed water and ethanol solvent at 22 °C. Numbers show time for which 2D J-aggregate was in contact with solvent. The intensity is normalized to the same scale, except for the bottom spectrum magnified by a factor of 12.

increasing content of Dye 2. Of course, Dye 2 may also form its own J-aggregates in the intermediate space, and eventually predominates the spectra when its molar percentage in solution exceeds ~80%. A series of spectra collected in Figure 3 indeed exhibits, together with a marked peak broadening, a systematic blue-shift of the J-band associated with Dye 1 with increasing content of the diluent. Furthermore the mixing also caused a noticeable blue-shift in the J-band of Dye 2 (normally at 575 nm; see the bottom spectrum in Figure 3). This in turn means that Dye 2 has no spectral contribution in the region longer than 600 nm, where all the spectral changes thus being due to the variation in the average size and/or the molecular ordering of the Dye 1 aggregate.

As mentioned above, Figure 3 shows that the additional J-band at ~570 nm, associated with the diluent, becomes very significant only after its molar percentage in the mixed dye solution exceeds ~80%, and grows rapidly thereafter to that for the 100% Dye 2 solution. In agreement with this behavior of the Dye 2 J-band, the integrated absorbance of the broadened J-band of Dye 1 suggests that there still remains more than half a monolayer coverage of Dye 1 even in the case of 80% Dye 2 solution. The surface coverage of Dye 1 thus decreases relatively slowly (not necessarily linearly) from 1 to ~0.6 monolayer as the molar percentage of Dye 2 in solution increases from 0 to ~80%. It is in this region, however, that a sufficiently large blue-shift occurs in the Dye 1 J-band. Further increase in the diluent concentration causes no further significant shift in the Dye 1 J-band, its limiting peak position being located at ~615 nm. This is likely to be associated with the smallest possible aggregate of Dye 1 to retain the characters of J-aggregate. Overall it is suggested that Dye 2 has a relatively low probability of being coadsorbed from the mixed dye solution, but yet achieves well the expected diluent function for Dye 1 to be constrained to form smaller 2D J-aggregates. It should be also stressed again that the main spectral change that we associate with the variation in the average aggregate size is the blue-shift in the J-band. Though the mixing also caused a marked peak broadening, it is mainly due to inhomogeneous broadening, which quite easily sets in by mixing of a minor amount of the diluent below 10% in solution.

The physical size difference between the 2D J-aggregates of Dye 1 formed in the absence and in the presence of Dye 2 is also reflected upon the changes of the respective absorption spectra in the course of solvent-induced molecular desorption (the corresponding kinetics will be discussed separately in a later section). Figure 4 shows an example of such spectral changes observed for the pure 2D J-aggregate of Dye 1 treated by mixed water and ethanol solvent. It can be seen that both the peak position and the bandwidth remain almost intact even after the intensity of the J-band has been diminished to less than 10% of the original intensity; i.e., after more than 90% of the originally adsorbed dye molecules have been lost into the solvent. This suggests that dye molecules are desorbed preferentially from the periphery of 2D dye islands, the residual smaller islands preserving the integrity as a 2D J-aggregate. Furthermore, according to the crude criterion that correlates the coherent size of a J-aggregate to the width of its J-band[27] (i.e., the extent of homogeneous broadening), the residual 2D J-aggregates shrunken to less than one tenth of the original size in Figure 4 and yet retaining a considerably sharp J-band, must still consist of tens of dye molecules in the lower limit (i.e., when the homogeneous broadening determines the bandwidth).

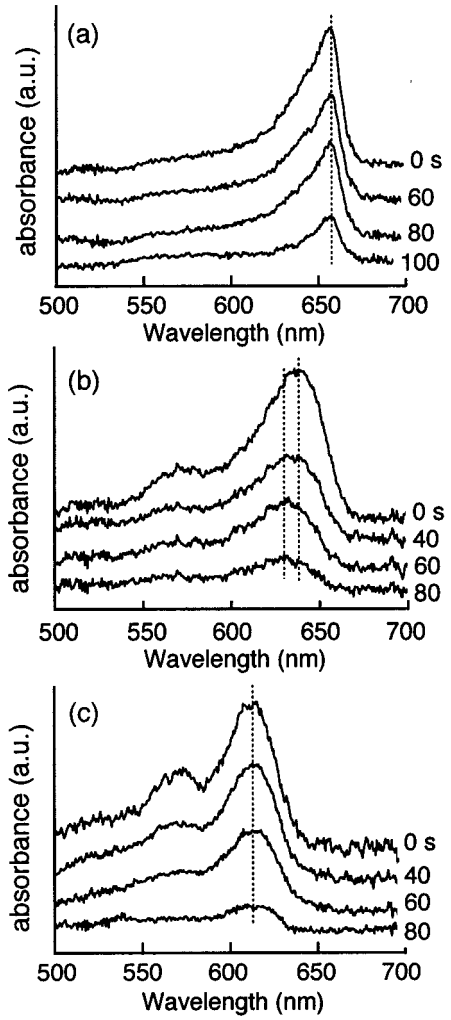

Figure 5. As in Figure 4 but for mixed assemblies of Dye 1 and Dye 2 adsorbed from mixed solutions with molar percentage of Dye 2 of (a) 5%, (b) 20%, and (c) 80%. The intensity is normalized to the same scale in each series.

If the observed bandwidth is also affected by inhomogeneous broadening, then the real physical size would become even greater. This means that each domain of 2D J-aggregate originally contained at least hundreds of dye molecules.

In contrast, in the case of mixed 2D assemblies of Dye 1 and Dye 2, molecular desorption therefrom caused notable changes also in the shape of the J-band as exemplified in Figure 5 for the conditions of lowest (5%), moderate (20%), and high (80%) molar percentage of Dye 2 in the mixed dye solution. In the first case (Figure 5 a), there is still a fair chance for some large 2D J-aggregates of Dye 1 to be formed along with much smaller ones. Because of this considerable size distribution and the tendency of smaller ones to dissolve faster, the composite J-band in this case apparently gets narrowed as the desorption progresses—the position of the main peak, only slightly different from that for the pure 2D J-aggregate, being virtually unaltered. In the intermediate region represented by Figure 5b, all the 2D J-aggregates of Dye 1 become so small that a net decrease in their average size by molecular desorption now manifests itself in a small but noticeable blue-shift in the peak position. Of course, as shown in Figure 5c, after the J-band peak has reached the aforementioned limiting position of ~615 nm, the molecular desorption causes no further blue-shift in the J-band.

3.2. XPS Analysis. It is obvious that a 2D J-aggregate of cyanine dyes can be formed only in such molecular configurations that allow plane-to-plane molecular stacking, thus excluding the flat-on adsorption. Then the estimated molecular area of Dye 1 in its 2D J-aggregate, ~80 Å^2, suggests that the dye molecules are closely packed in the edge-on configuration with the molecular long axis parallel to the substrate surface. Even so it is still not clear in which one of the two opposite vertical orientations the dye molecules are sitting on the bromide monolayer. The XPS analysis, first of all, gives us a definite answer to this question through a series of angle-resolved XPS spectra, of which a typical example is shown in Figure 6 for the S_{2p} core levels. Here the left-hand peak at a higher binding energy comes from the S atoms in the sulfonic acid groups, while the other one appearing at a lower binding energy arises from the S atoms in the heterocyclic ring of the main dye chromophore. That these two kinds of S atoms are clearly distinguishable by XPS in terms of the core-level binding energy is a major advantage of Dye 1 for the present work.

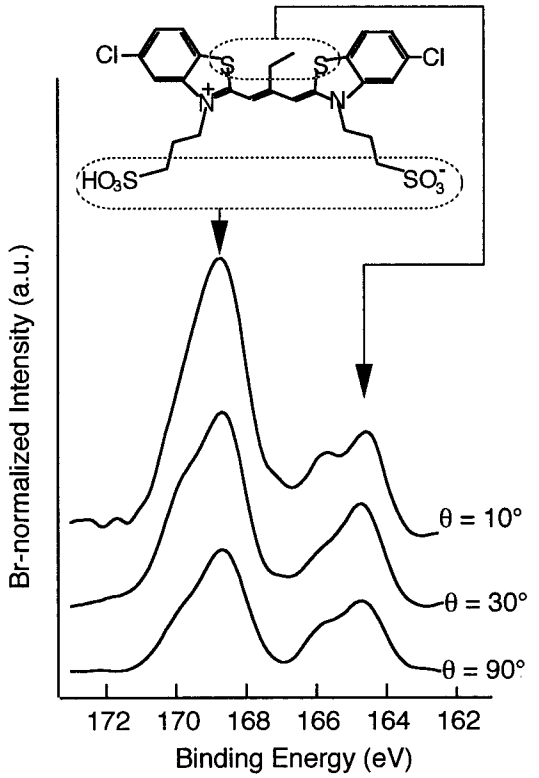

Figure 6. Angle-resolved XPS spectra for S_{2p} core levels measured for 2D J-aggregate of Dye 1 at photoemission angles of 10°, 30°, and 90° with respect to the sample plane. The intensity is normalized by that of the Br_{3p} signal arising from the underlying bromide monolayer to correct for the angle-dependent instrumental factors.

In Figure 6 it can be seen that the relative intensity of the left-hand signal increases significantly with decreasing photoemission angle (defined with respect to the sample plane), whereas the right-hand one exhibits only minor angle dependence. A large angle dependence comparable to that of the former signal in Figure 6 was also found in the O_{1s} spectrum, which is another signal arising from the sulfonic acid groups, and minor angle dependence was common to the atoms (S, N, and Cl) contained in the main dye chromophore. Note that the signal intensity here is normalized by the intensity of the Br_{3p} signal associated with the bromide monolayer underneath the 2D J-aggregate to compensate for the angle-dependent instrumental factors. Then smaller angle dependence in the given signal means that the corresponding atoms are closer in depth to the bromide monolayer. The observed angle dependencies in the XPS signals thus unambiguously tell us that Dye 1 is

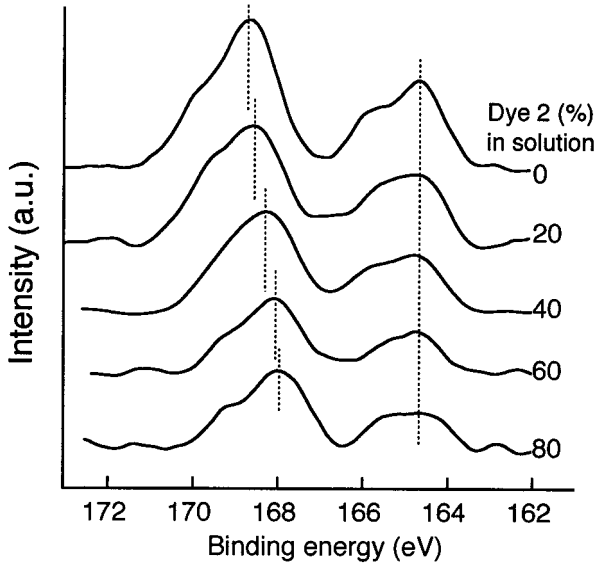

Figure 7. S_{2p} core-level XPS spectra taken for mixed 2D assemblies of Dye 1 and Dye 2 adsorbed from mixed dye solutions with various molar percentages of Dye 2. Compare with Figure 3 for the corresponding absorption spectra.

adsorbed in the orientation with the cationic chromophore facing the bromide monolayer and the sulfonic acid groups being outside the dye cation layer at a distance controlled by the length of the propyl chain.

The above result of the angle-resolved XPS also supports that Dye 1 is adsorbed with its standard conformation that has been assumed in Figure 1. Besides this structure, cis−trans isomerization at the methine chain may also allow Dye 1 to take an opposite conformation in which the two sulfopropyl groups and the meso ethyl group are all brought to the same side of the molecule. In this alternative geometry, however, not only some considerable steric congestion is caused around the meso-ethyl group, but the two Cl atoms come too much closer to the sulfonic acid groups (and thus too much away from the bromide monolayer) to be consistent with the minor angle dependence of the Cl signal.

Clear distinction between the sulfonic acid groups and the main dye chromophore including the Cl atoms also occurs with respect to the following XPS information more vital for the present work; namely a unique and systematic chemical shift in the core-level binding energies associated with the sulfonic acid groups relative to those with the cationic dye chromophore. Figure 7 shows a series of S_{2p} spectra taken for a variety of 2D assemblies of Dye 1 of which the average aggregate size was controlled by mixing Dye 2 in the parent dye solution; the corresponding absorption spectra were already shown in Figure 4. Figure 7 indicates that all the right-hand peaks originated from the dye chromophore are aligned at the same position in binding energy (164.7 eV) when the N_{1s} signal (401 eV), arising also from the dye chromophore, is used as the common energy reference. This was also the case with the Cl_{2p} signal, invariably located at 201 eV. In contrast, the positions of the left-hand peaks in Figure 7 exhibit a systematic chemical shift—farthest from the right-hand peak (largest in binding energy; 168.7 eV) for the pure 2D J-aggregate and getting closer to the right-hand peak as the average aggregate size is decreased, eventually converging at 168 eV. It would be worth noting that the spectrum at this stage was indistinguishable from that which was independently taken for a powder sample of Dye 1. It was confirmed that the binding energy of another signal (O_{1s}) representative of the sulfonic acid groups also moved in parallel to the left-hand peak of the S_{2p} signal as expected.

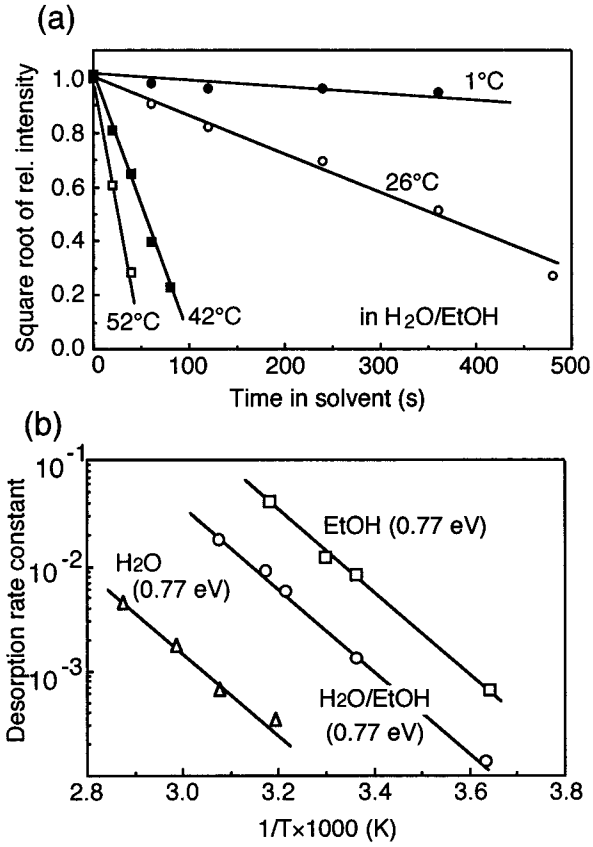

Figure 8. (a) Linear relationship between square root of residual J-band intensity and time in solvent observed by solvent-induced molecular desorption from 2D J-aggregate of Dye 1. The solvent is mixed water and ethanol of 1:1 volume ratio. (b) Arrhenius plots of apparent desorption rate constants, defined by the slopes of the lines in (a), for three different kinds of solvents.

The "intramolecular" chemical shift, nearly 1 eV at maximum, observed for the same dye molecules but in different sizes of 2D J-aggregates is quite unique and seems to be rationalized only in terms of some significant Madelung potential that occurs in a close-packed 2D dye assembly consisting of cationic dye chromophores and counteranions. If so, this electrostatic interaction must be a major contributor to the overall cohesive energy of 2D J-aggregate, which would otherwise be stabilized only by the short-range van der Waals interactions. Before discussing the correlation of this collective Coulomb interaction energy with the molecular arrangement and with the 2D aggregate size, let us next examine how the cohesive energy of 2D J-aggregate is reflected upon the kinetics of the solvent-induced molecular desorption.

3.3. Desorption Kinetics. We have suggested already that the molecular desorption from the 2D J-aggregate put in a dye solvent preferentially occurs from the periphery of 2D dye islands. This is supported also by the corresponding kinetics of desorption, as inferred from the way the intensity of the J-band decreases as a function of time in dye solvent. Namely as seen in Figure 8a the relationship between the square root of residual J-band intensity and the time in solvent shows a good linearity over the wide range, irrespective of the solvent temperature. The proposed desorption mode reasonably accounts for this behavior, as the number of dye molecules forming the periphery of 2D dye islands, which determines the desorption rate, is expected to be proportional to the square root of the total number

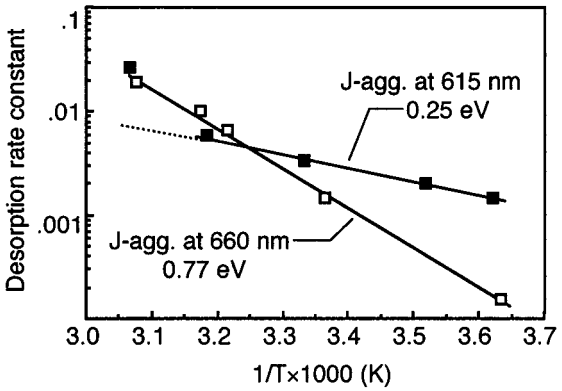

Figure 9. Comparison between pure 2D J-aggregate (J-band at 660 nm) of Dye 1 and that heavily broken up by Dye 2 (J-band at 615 nm; formed at 80% diluent level in solution) in terms of the temperature dependence of the apparent desorption rate constant in mixed water and ethanol solvent of 1:1 volume ratio.

of dye molecules left on the substrate, i.e., the residual J-band intensity. It should be also noted that the amount of dye solvent used in these experiments was chosen so that even complete desorption of all the dye molecules on the substrate keeps the corresponding dye concentration in the solvent below 10^{-10} M. The observed kinetics is thus considered not to be affected by readsorption of the dissolved dyes. Dye aggregation in the solvent is also improbable even in the case of pure water solvent.

The slope of each line in Figure 8a then serves as a measure for the effective rate constant for the molecular desorption at each solvent temperature. A series of Arrhenius plots of this kinetic parameter for the three different kinds of solvents is as shown in Figure 8b. Interestingly, all the lines in Figure 8b are parallel to each other, giving an equal activation energy of 0.77 eV. Note, however, that the absolute rate of desorption strongly depends on the kind of solvent, varying by as much as 3 orders of magnitude from the smallest value in water to the largest one in ethanol. This suggests that the transition state of desorption is little stabilized in energy by solvation, but the transition entropy, or the frequency factor, is markedly increased with increasing content of ethanol in the solvent.

With this particular nature of the transition state in mind, it seems that the measured activation energy in Figure 8 gives a crude estimate of the molar cohesive energy of 2D J-aggregate (this of course includes the contribution by dye−substrate interaction), which refers to isolated monomers rather than to those in the bulk of the solvent. It should be also stressed that the required energy to remove one molecule from the periphery of 2D dye island, where the dye molecules are not fully surrounded by other molecules, may not considerably be different from the real molar cohesive energy. This is because removal of an arbitrary molecule from the periphery makes an adjacent inner molecule take over the peripheral position simultaneously, and the final state is equivalent to that resulting from a hypothetical removal of an internal molecule followed by vacancy migration to the periphery.

To figure out what fraction of the apparent activation energy, 0.77 eV, represents the electrostatic contribution, it is useful to compare again the pure 2D J-aggregate of Dye 1, for which the J-band is located at 660 nm, and the one broken up by Dye 2 to the level where the limiting position of the J-band (615 nm) is reached. According to Figure 7, the intramolecular chemical shift between these two kinds of J-aggregates amounts to ∼0.7 eV, which serves as a measure for the difference in the collective Coulomb interaction energy per molecule. Figure 9 shows a comparison between two Arrhenius plots of the effective desorption rate constants for the corresponding two samples in the mixed water and ethanol solvent. Here the broken-up J-aggregate was prepared at the 80% diluent level in the mixed dye solution. A similar result was obtained also for pure water, but in pure ethanol the desorption from the broken-up J-aggregates was too fast to follow. As for the concurrent desorption of the diluent (Dye 2) and its potential influence on the desorption kinetics of Dye 1 we first refer to Figure 5c, which shows that the Dye 2-related additional J-band is attenuated noticeably faster than the main J-band at 615 nm. This means that the Dye 1:Dye 2 molar ratio in the mixed assembly varies with time in solvent. The fact that we could nevertheless assign a time-independent effective desorption rate constant for Dye 1 (as plotted in Figure 9) suggests that the desorption from the broken-up J-aggregate of Dye 1 was kinetically independent of the desorption of Dye 2 from the intermediate space. This would be a reasonable behavior unless the partial desorption of Dye 2 can extensively cause some substantial reorganization of the broken-up J-aggregates of Dye 1 into larger, more uniform aggregates; a process not agreeable with the time-independent peak position of the J-band at the limiting 615 nm as shown in Figure 5c.

In Figure 9 it can be seen that a considerably smaller activation energy of 0.24 eV is associated with the broken-up J-aggregates, except for the high-temperature region (>40 °C) beyond the point where the two lines intersect with each other. There, some more drastic mode of desorption probably sets in for the broken-up J-aggregates. Note that the difference between the above two values of activation energy, more than 0.5 eV, is comparable to the magnitude (∼0.7 eV) of the intramolecular XPS chemical shift. This suggests that the main part of the 0.77 eV activation energy for sufficiently large 2D J-aggregates has indeed an electrostatic origin. Given that the apparent activation energy for desorption reflects a major fraction of the molar cohesive energy, as suggested already, the result also indicates that the predominant contribution to the molar cohesive energy comes from the collective Coulomb interaction involving dye cations and counteranions. Overall we predict the molar cohesive energy of 2D J-aggregate of Dye 1 to be of the order of 1 eV including other, relatively minor, contributions by the short-range van der Waals interactions between dye molecules and also by the interaction between the substrate and the respective dye molecules, i.e., the molar adsorption energy. In a first approximation these additional contributions would be independent of the aggregate size.

3.4. Molecular Arrangement of the 2D J-Aggregate. The significance of the electrostatic energy for the 2D molecular assembly of cyanine dyes is not only to stabilize the 2D dye network but also to give strong constraint with respect to the allowed molecular arrangement. A semiquantitative argument of this effect can be made by introducing several, more-or-less crude assumptions to simplify the problem.

First, in accordance with the estimated molecular area of 80 Å^2 and also with the edge-on configuration proved by the angle-resolved XPS, we assume that dye molecules are arranged periodically at fixed regular spacings of 20 and 4 Å, respectively, along and normal to the molecular long axis. Then the slip angle is the only adjustable parameter for the molecular arrangement. Both of the assumed spacings seem reasonable in view of the approximate length of the molecule, ∼17 Å, in the conformation shown in Figure 1 and the graphitic plane-to-plane distance of 3.5 Å. Next we replace the delocalized positive charge associated with the cationic dye chromophore by a point charge collected

at its center—an assumption most crude of all but essential for simplifying the numerical simulation. Finally, in the edge-on configuration, the counter negative charge in the form of sulfonate anion is a little arbitrarily fixed laterally on one end of the molecule 9 Å away from the molecular center and vertically 3.5 Å above the point positive charge. In practice, in a 2D dye assembly with the above-assumed molecular spacings, there is a way to make the two sulfonic acid groups on each molecule equivalent with each other, both carrying half the counter negative charge. This is realized by bridging two adjacent sulfonate anions on two neighboring molecules lined up along the molecular long axis with either a proton or a triethylammonium ion[28] (cf. Figure 1). However, the resultant difference from the former model is only trivial in that a formal unit negative charge, now carried by the two bridged groups together, is located in the middle of the two neighboring molecules, just a little farther away from the molecular center.

The collective Coulomb interaction energy per molecule, or the Madelung energy, for an arbitrary aggregate can be calculated by using the total sum method, wherein all the individual cation−cation, anion−anion, and cation−anion interactions except for the intramolecular cation−anion interactions are summed up and then the result is divided by the total number of molecules. In the case of sufficiently large aggregates comprising, for example, hundreds of dye molecules or more, the same energy may be approximated by the partial sum accounting for the interactions between the central dye cation and all the other dye cations and counteranions except for the counteranion on the central molecule. Figure 10a shows the relationship between the thus (by the partial sum method) calculated Madelung energy and the slip angle for a sufficiently large 2D assembly consisting of a few thousand dye molecules. It can be seen that attractive interaction occurs only in a limited region of relatively low slip angle and gets rather sharply maximized at ∼20°, where the so-called brickstone arrangement shows up.

For further reference, we have also calculated the size dependence of the electrostatic stabilization energy per molecule for the size range corresponding to 2−225 molecules by using the total sum method. We have first confirmed that the maximum stabilization for these smaller aggregates also occurs at ∼20° slip angle. Figure 10b then shows how this energy depends on the aggregate size for a fixed slip angle of 21.8°, corresponding to the most stable symmetric brickstone arrangement. The inset shows the top views of a couple of small 2D dye units (containing 4 or 9 dye molecules) modeled in this calculation; similar symmetric aggregate shapes were assumed for all the larger sizes. It can be seen that the electrostatic stabilization energy per molecule increases with increasing aggregate size as expected. It is considered that the systematic XPS chemical shift shown in Figure 7 is what experimentally mirrors this size dependence in the electrostatic cohesive energy for the 2D J-aggregate. More specifically, the calculated size dependence in Figure 10b is particularly significant for small aggregates containing less than 20 molecules, being gradually leveled off for larger aggregates. Provided that the calculated electrostatic energy scales approximately linearly to the intramolecular XPS chemical shift shown in Figure 7 and that the pure 2D J-aggregate (peaked at 660 nm) of Dye 1 consists of at least hundreds of dye molecules or more, then we can even back-estimate the average aggregate size of Dye 1 in the mixed 2D assembly. Namely, for the diluent percentages in solution, 20%, 40%, and 60−80% (corresponding to 640, 630, and 621−615 nm, respectively, in the peak position of the Dye 1 J-band), each aggregate is estimated to comprise ∼100, ∼10, and a few to several dye molecules on the rough average.

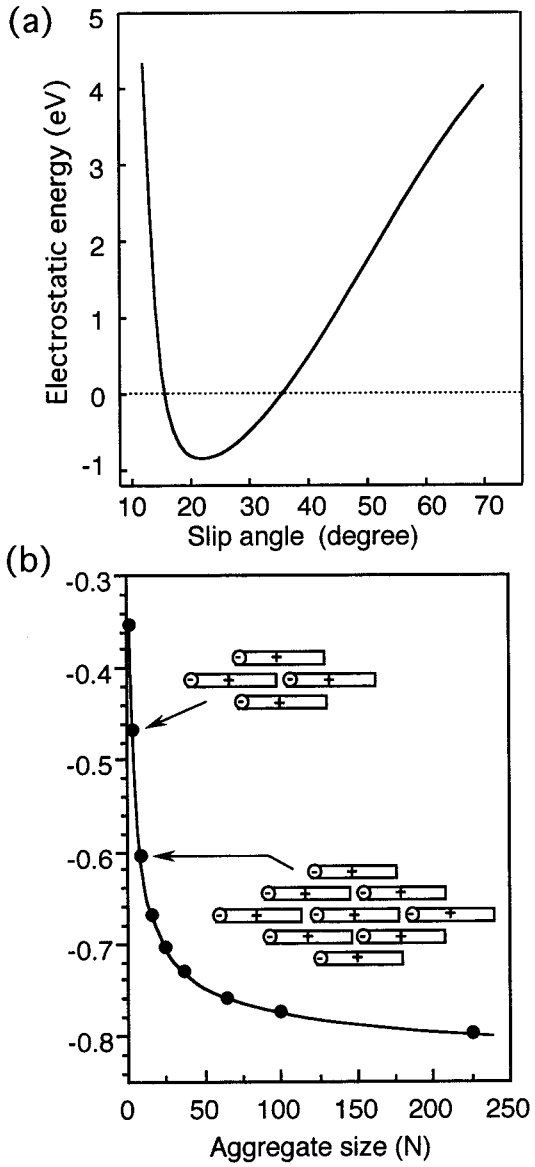

Figure 10. (a) Simulated electrostatic energy as a function of slip angle for 2D assembly of Dye 1 consisting of a few thousand dye molecules, arranged at regular spacings 20 and 4 Å, respectively, along and normal to the molecular long axis. Calculated by partial sum method. See text for more detail. (b) Size dependence of electrostatic energy for relatively small 2D J-aggregates of Dye 1 calculated by direct sum method at a fixed slip angle of 21.8°. For reference, the inset shows top views of a couple of small dye units modeled in this calculation.

Though crude in absolute terms, the present numerical simulation thus testifies to the critical role of the electrostatic interactions to make predominant contribution to the molar cohesive energy and to essentially determine the allowed molecular arrangement or slip angle. Note, however, that the electrostatics never controls the aggregate size—larger ones always being thermodynamically favored. Thus, the actual aggregate size that occurs in each different system is controlled by kinetic factors for the aggregate formation or, in the case of mixed dye assembly, by physical interference against homogeneous growth.

It should be also noted that in the framework of the point-charge approximation the assumed 2D dye network does not necessarily give the maximum electrostatic stabilization. In practice pseudo-one-dimensional brickstone aggregates, which

consist of just two lines of plane-to-plane stacked molecules along the molecular long axis, acquire a substantially greater stabilization than that in the real 2D assembly. This can be understood by realizing that, in the 2D brickstone arrangement, molecules appearing in every other two lines along the molecular long axis are arranged relative to one another at a large slip angle of 90°. The minimum distance between the centers of these molecules is only twice the primitive spacing (assumed to be 4 Å in our model) normal to the molecular long axis, and thus the cation−cation and anion−anion interactions for these molecules give significant repulsive contribution to the overall cohesive energy. The point charge approximation for dye cations probably overestimates this repulsive component, however. Furthermore, the short-range van der Waals interactions also contribute to the cohesive energy, stabilizing the 2D aggregate to a greater extent than for the pseudo-one-dimensional arrays. Overall we expect that the 2D J-aggregate favors a real 2D dye network, which agrees also with the kinetics of desorption discussed in the previous section.

We finally emphasize that the large contribution of the electrostatic energy for 2D J-aggregation should not be associated with the particular structure of Dye 1 having counteranions fixed to the cationic dye chromophore. For example, a similar XPS analysis of the 2D J-aggregate of Dye 2, having counteranions (chloride ions) physically separable from the dye chromophore, also proved a significant chemical shift in the core-level binding energy associated with the counteranions relative to that for the dye cation, as compared to a powder sample. The only problem with this type of dye is that the position of the counteranion relative to the dye cation in the 2D dye assembly is not so clearly specified as in the case of Dye 1, thus requiring an extra thought in interpreting the experimental results.

4. Conclusion

Atomically flat Ag(111) films covered with a halide monolayer, a pseudo AgX(111) model surface, allows well-ordered 2D J-aggregates of cyanine dyes to be easily self-assembled from a dilute monomeric dye solution.

The structural simplicity of the system makes XPS a powerful tool to study not only the vertical molecular orientation in the 2D J-aggregate but also what essentially controls the lateral molecular arrangement. In particular, a unique "intramolecular" chemical shift in the core-level binding energy between the cationic dye chromophore and the counteranion, which varied systematically with the average aggregate size, uncovered for the first time a significant Madelung potential that stabilizes the 2D molecular network of a typical cyanine dye.

The significance of this electrostatic energy has been supported further by the kinetic analysis of solvent-induced molecular desorption from the 2D J-aggregate, accounting for the major part of the overall molar cohesive energy of the 2D J-aggregate that probably reaches ∼1 eV including the relatively minor contributions by the short-range van der Waals interactions. In addition, this long-range Coulomb interaction is a sensitive function of the molecular arrangement, forcing the corresponding slip angle to fall in a limited range favorable for the occurrence of a sharp J-band.

References and Notes

(1) West, W.; Gilman, P. B. *The Theory of the Photographic Process*, 4th ed.; James, T. H., Ed.; Macmillan: New York, 1977; Chapter 10.
(2) Bohn, P. W. *Annu. Rev. Phys. Chem.* **1993**, *44*, 37.
(3) Möbius, D. *Adv. Mater.* **1995**, *7*, 437.
(4) Daehne, S.; De Rossi, U.; Moll, J. *J. Soc. Photogr. Sci. Technol. Jpn*. **1996**, *59*, 250.
(5) Wang, Y. *Chem. Phys. Lett.* **1986**, *126*, 209.
(6) Spano, F. C.; Mukamel, S. *Phys. Rev. A.* **1989**, *40*, 5783.
(7) Norland, K.; Ames, A.; Taylor, T. *Photogr. Sci. Eng.* **1970**, *14*, 295.
(8) Mako, S.; Kanamaru, N.; Tanaka, J. *Bull. Chem. Soc. Jpn*. **1980**, *52*, 3120.
(9) Matsubara, T.; Tanaka, T. *J. Imaging Sci*. **1991**, *35*, 274.
(10) Czikkely, V.; Försterling, H. D.; Kuhn, H. *Chem. Phys. Lett*. **1970**, *6*, 11.
(11) Bücher, H.; Kuhn, H. *Chem. Phys. Lett*. **1970**, *6*, 183.
(12) Duschl, C.; Frey, W.; Knoll, W. *Thin Solid Films* **1988**, *160*, 251.
(13) Mizrahi, V.; Stegeman, G. I.; Knoll, W. *Phys. Rev. A.* **1989**, *39*, 3555.
(14) Wolthus, L.; Schaper, A.; Möbius, D. *Chem. Phys. Lett*. **1994**, *225*, 322.
(15) Kawasaki, M.; Ishii, H. *Langmuir* **1995**, *11*, 832.
(16) Kawasaki, M.; Ishii, H. *J. Imaging Sci. Tech*. **1995**, *39*, 210.
(17) Kawasaki, M.; Uchiki, H. *Surf. Sci.* **1997**, *388*, L1121.
(18) Kawasaki, M. *Appl. Surf. Sci.* **1998**, *135*, 115.
(19) Lanzafame, J. M.; Muenter, A. A.; Brumbaugh, D. V. *Chem. Phys.* **1996**, *210*, 79.
(20) Asanuma, H.; Tani, T. *J. Phys. Chem. B.* **1997**, *101*, 2149.
(21) Kirstein, S.; Möhwald, H.; Shinomura, M. *Chem. Phys. Lett*. **1989**, *154*, 303.
(22) Yonezawa, Y.; Miyama, T.; Ishizawa, H. *J. Imaging Sci. Technol*. **1995**, *39*, 331.
(23) Born, M.; Wolf, E. *Principles of Optics*, 5th ed.; Pergamon Press: Oxford, 1975; Chapter 7.
(24) Born, M.; Wolf, E. *Principles of Optics*, 5th ed.; Pergamon Press: Oxford, 1975; Chapter 12.
(25) *Handbook of Optical Constants of Solids*; Palk, E. D., Ed.; Academic Press: Orlando, 1985; p. 354.
(26) Smith, D. L. *Photogr. Sci. Eng.* **1974**, *18*, 309.
(27) Knapp, E. W. *Chem. Phys*. **1984**, *85*, 73.
(28) According to careful comparisons between various XPS signals taken for the 2D J-aggregate of Dye 1 in terms of the integrated intensity corrected for the sensitivity factor, the total intensity of the N_{1s} signal was a little too large to attribute to just the two N atoms in the main dye chromophore. The extra intensity is considered to come from the triethylammonia or ammonium ion in the batainic structure of Dye 1 shown in Figure 1.